JOURNAL OF MATERIALS SCIENCE 31(1996) 3145–3151

Natural ageing behaviour of cast alumina particle-reinforced 2618 aluminium alloy

I. N. A. OGUOCHA, S. YANNACOPOULOS*
Department of Mechanical Engineering, University of Saskatchewan, Saskatoon, Canada S7N 0W0

The effect of the presence of 10 and 15 vol% alumina particles on the natural ageing behaviour of cast 2618 aluminium alloy was investigated using microhardness measurements and differential scanning calorimetry. It was found that the addition of the alumina particles does not alter the ageing sequence of 2618 Al although certain aspects of the precipitation reactions are changed. In particular, the relative quantities of the various phases were changed by reinforcement addition. Increasing the alumina content decreased the volume fractions of the Guinier–Preston–Bagaryatskii (GPB) I phases. Also, the peak reaction temperature, (T_p), for the GPBII and S′ phases decreased with increasing volume fraction of alumina.

1. Introduction

Aluminium alloys reinforced with SiC and alumina (Al_2O_3) particles have emerged as the most used and investigated discontinuous metal matrix composites (MMCs). They are currently used in the small production of bicycle parts [1] and are strongly being considered for futuristic automobile parts, such as connecting rods, pistons, and brake discs, as well as for aircraft static structures [2, 3], advanced composite optical-system gimbals [3], and in microwave and microelectronics packaging components [4]. Unlike the continuous fibre-reinforced MMCs, the properties of the matrix of a discontinuously reinforced MMC influence the ultimate and yield strength values of the composite. At present, most of the alloys employed as matrices in this class of MMCs are age-hardenable aluminium. Usually, the assumption is made that the ageing characteristics of these alloys are unaffected by the presence of the ceramic reinforcement, probably, because the strengthening whiskers or particles, such as SiC and alumina, are relatively inert phases, which are not expected to alter greatly the overall chemistry of the matrix alloy. However, sufficient evidence now exists in the open literature which indicates that the presence of the reinforcing whiskers or particles affects precipitation reactions and precipitate morphology in MMCs [5, 6].

The addition of a reinforcing ceramic phase to a metal alloy significantly increases the dislocation density in the matrix upon cooling from the solution heat-treatment temperature. The density of dislocations is increased mainly due to a large difference in the coefficients of thermal expansion of the ceramic reinforcement and the matrix, which generates thermal stresses usually large enough to deform the ductile matrix plastically. The dislocations which are created at the matrix–reinforcement interface and also in the matrix can affect the latter in two ways: (i) in a non-age-hardenable alloy, they give rise to simple dislocation strengthening [7], and (ii) in an age-hardenable alloy, they can act as heterogeneous nucleation sites for the precipitates during ageing of a MMC [8]. As such, dislocations can alter the precipitation kinetics in the matrix of a MMC. In the present study, the effect of alumina particles on the natural ageing behaviour of cast 2618 aluminium have been evaluated by means of microhardness measurements and differential scanning calorimetry (DSC) techniques.

2. Experimental procedure

2.1. Materials

Alumina particle-reinforced 2618 aluminium composites (10 and 15 vol %) and unreinforced 2618 aluminium were received from Duralcan Aluminium Company (San Diego), USA. The composites were fabricated by a proprietary casting method. Unreinforced 2618 Al alloy, was used as a reference material. The chemical compositions of the three materials are shown in Table I.

The samples of the unreinforced and 10 vol % Al_2O_3/2618 Al materials used for microhardness measurements were cut from extruded rectangular bars of these materials, measuring 20 mm × 20 mm × 5 mm in size. For the 15 vol % Al_2O_3/2618 Al composite, the samples were cut from cylindrical bars, 12.8 mm in diameter. The DSC samples were cut from cylindrical bars and measured approximately 5.6 in diameter. All samples were solution heat

*Author to whom all correspondence should be addressed.

TABLE I Chemical compositions of test materials

Material	Element[a]									
	Si	Fe	Cu	Mn	Mg	Cr	Ni	Zn	Ti	Al_2O_3[b]
2618 Al	0.18	1.19	2.34	–	1.59	–	1.05	–	0.07	–
2618 + 10	0.17	1.15	2.15	0.01	1.69	0.002	1.08	0.02	0.07	9.3
2618 + 15	0.18	1.09	2.11	0.01	1.53	0.004	1.04	0.02	0.07	15.7

[a] Balance = Al.
[b] Composition in vol %; the rest in wt %. 2618 Al = 2618 Al alloy; 2618 + 10 = 10 vol % Al_2O_3/2618 Al composite; 2618 + 15 = 15 vol % Al_2O_3/2618 Al composite.

treated for 2 h at 530 ± 2 °C in a constant-temperature air furnace, followed by quenching in laboratory water and natural ageing at room temperature.

The microhardness samples were metallurgically polished using 6 μm grade diamond paste. Vickers hardness measurements were then carried out on the polished samples using a Buehler Microhardness tester (Micromet II) with a 50 g direct load applied for 15 s. The small load was chosen in order to produce indentations small enough to occur only in the matrix and away from the particles in the plane of measurement. At least 11 approximately equally spaced microhardness measurements were made for each specimen to ensure representative results. The presence of any subsurface particles and voids was identified by the excessively high and low hardness values, respectively.

DSC analyses of solution heat-treated samples were carried out using a Mettler TA 4000 thermal analyser with a plug-in Mettler DSC-20 cell. At least, two DSC runs were conducted in order to ensure reproducibility. All DSC runs began at 30 °C and ended at 530 °C with a constant heating rate of 10 °C min^{-1}. The built-in evaluation algorithms were used for calculation of all specific heat results. In order to correct for the additional heat flow arising from the difference in weight of sample pan and reference pan, and also to compensate for any asymmetry in the measuring system, a preliminary blank experiment was performed with commercially pure aluminium and thus the heat flow used in specific heat evaluations was the difference between the measured and blank values. The specific heat data were normalized for unit mass of the metal matrix in order to remove the contributions of alumina particles to heat flow.

3. Results and discussion

3.1. Microhardness

Fig. 1 shows the variation of matrix microhardness as a function of ageing time for both unreinforced and reinforced 2618 aluminium alloys aged at room temperature for up to 500 h. The natural ageing response of the three materials shows a similar trend: the hardness increases initially with increasing ageing time up to an initial maximum after which it decreases briefly with further ageing time, and then increases monotonically with further ageing. Thus the overall ageing sequence in unreinforced 2618 aluminium is not changed by the addition of alumina particles.

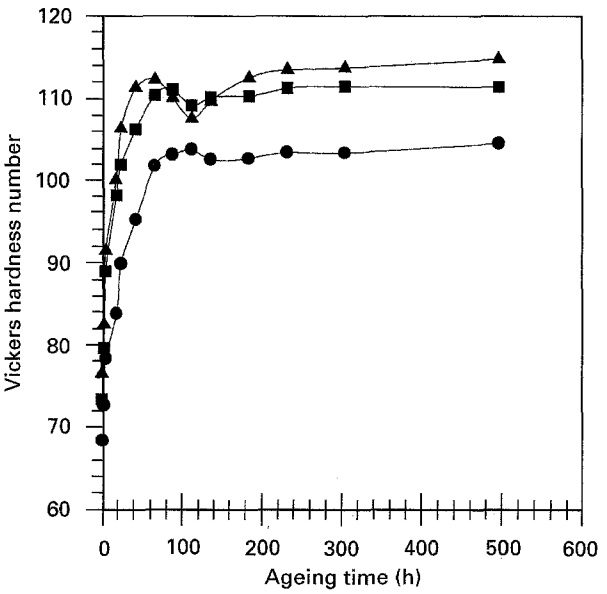

Figure 1 Microhardness as a function of ageing time at room temperature. (●) 2618 Al, (■) 2618 + 10, (▲) 2618 + 15.

However, a few features of Fig. 1 are noteworthy. First, the as-quenched matrix microhardness increases with increasing alumina content. Secondly, the attainment of the initial maxima in the hardness values occurs earlier in the composites, relative to the unreinforced metal matrix, suggesting that some aspects of the natural ageing kinetics of 2618 aluminium alloy are altered or enhanced by the presence of the alumina particles. Thirdly, the microhardness values of the composite matrices start out higher than that of the unreinforced alloy and remain higher up to the end of the 500 h test period.

Although the details of the precipitation sequence of Al–Cu–Mg alloys, to which 2618 aluminium alloy belongs, are yet to be fully understood, the sequence of phase transformations during ageing of the supersaturated solid solutions most often [9–11] follow the sequence

$$SSS \rightarrow GPBI \rightarrow GPBII(S'') \rightarrow S' \rightarrow S(Al_2CuMg) \quad (1)$$

where SSS = supersaturated solid solution, GPB = Guinier–Preston–Bagaryatskii zones, S″ and S′ phases are intermediate phases between the supersaturated solid solution and the equilibrium S phase. In these alloys, it has been reported that natural ageing occurs by the growth of the GPB zones [9], which

are copper/magnesium-rich clusters in the matrix. The hardness curves shown in Fig. 1 do not display any overageing behaviour within the time period tested. Therefore, it can reasonably be assumed that the majority of precipitates are of the coherent and semicoherent types. The coherent precipitates (GPB zones) cause, initially, an increase in hardness as a result of the distortion of the aluminium alloy matrix lattice which sets up large strain fields in the vicinity of the precipitates which, consequently, impede the movement of dislocations. This soon attains a maximum. At this stage, some of the GPBI zones change their morphology [12] via a complex reversion process. It is possible that such a transformation causes some momentary decrease in hardness and hence the observed hardness trough which is more pronounced at high alumina content. Subsequently, with the appearance and growth of GPBII precipitates, there is a further increase in hardness due to increased internal stresses. With further ageing, these precipitates grow in size and gradually lose their degree of coherency with the matrix and, consequently, the rate of increase in hardness slows down.

The higher hardness observed in the reinforced 2618 aluminium and the apparently enhanced ageing response can be associated with the enhanced dislocation substructure and quenched-in vacancy loops formed during cooling from the solution treatment temperature. The matrix of the composite has a larger portion of strained regions and hence density of dislocations. The dislocation networks result in increased internal stresses and, hence, higher hardness of the composite matrix relative to that of the unreinforced matrix. Further, there is a possibility of additional strength coming from the transition phases (e.g. S′) during natural ageing, especially in the composite materials, because it has been shown that S′ phase nucleates preferentially upon dislocation loops and helices, and quenched-in vacancy loops during quenching [10, 13].

The apparent acceleration of the natural ageing process in the composites can be explained also in terms of the difference between the thermal conductivities of the alumina particles and the matrix (Al_2O_3: $C_p = 765\ J\,kg^{-1}\,K^{-1}$; $\kappa = 36.0\ W\,m^{-1}\,K^{-1}$ versus aluminium: $C_p = 903\ J\,kg^{-1}\,K^{-1}$; $\kappa = 237\ W\,m^{-1}\,K^{-1}$, all at 300 °C [14]). This can produce significant microscopic thermal gradients within the composite materials during quenching from the solution heat-treatment temperature. The matrix in the immediate vicinity of the alumina particles will be at a higher temperature than the alloy matrix away from the reinforcement–matrix interface. Consequently, solute atoms will migrate to these interfaces of higher solubility, their diffusion being assisted by the increased thermal activation in these regions. Because there are more strained regions in the composites than in the unreinforced matrix, the distance through which the solute atoms will traverse to reach favourable nucleation sites will be reduced [15]. The distorted regions will also tend to promote strain-induced solid-state diffusion of solute atoms and vacancies to the reinforcement–matrix interface in an attempt to reduce or annihilate the misfit strains in the lattice.

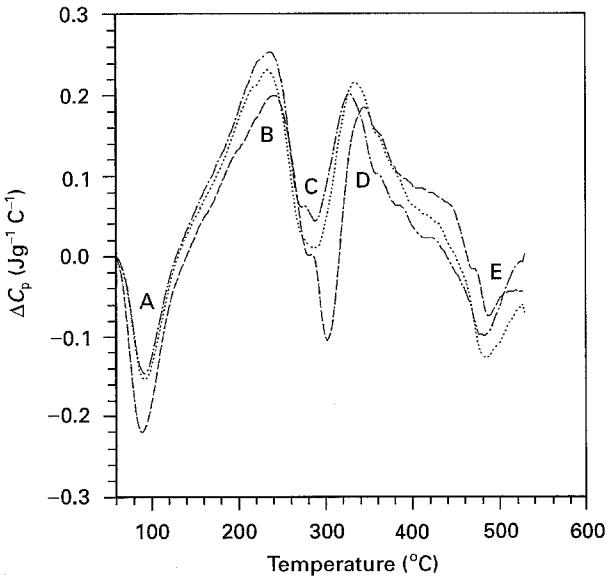

Figure 2 DSC thermograms of the reference alloy and the composites in the as-quenched condition. (——) 2618 Al, (-----) 2618 + 10, (– – –) 2618 + 15.

3.2. Differential scanning calorimetry

3.2.1. As-quenched condition

Fig. 2 shows the differential specific heat versus temperature curves for unreinforced 2618 Al, 10 vol % Al_2O_3/2618 Al, and 15 vol % Al_2O_3/2618 Al in the as-quenched condition. The principal features of the DSC thermograms shown in Fig. 2 have been labelled A–E. It is evident that the three materials show the same general characteristic reaction regions which can be identified [5, 16] as:

(i) an exothermic precipitation reaction (A) between 60 and 130 °C;

(ii) an endothermic dissolution reaction (B) between 130 and 260 °C;

(iii) a doublet exothermic precipitation reaction (C) between 260 and 315 °C;

(iv) an endothermic dissolution reaction (D) between 315 and 410 °C; and

(v) an exothermic precipitation reaction (E) between 410 and 530 °C.

These temperature intervals are based on the unreinforced matrix alloy alone and are only approximate, because it is very difficult to identify the exact transition points both manually and with the help of an integration package supplied with the thermal analyser. Hence, the overall precipitation sequence of 2618 alloy is not changed by the addition of Al_2O_3 particles but certain aspects of the reactions are different.

A number of studies have shown that zone formation in Al–Cu–Mg alloys takes place at room temperature in the as-quenched condition [5, 10, 11, 17, 18]. Cho [19] has reported that the rate of GPB zone formation in an Al–2.0 wt % Cu–1.1 wt % Mg alloy is maximum between 70 and 120 °C, while Papazian [5] has documented that the formation of GPB zones

TABLE II Peak reaction temperature of DSC thermograms for samples tested in the as-quenched condition

Material	Peak A (°C) (GPB formation)	Peak B (°C) (GPB dissolution)	Peak C (°C) (S′/θ′ formation)	Peak D (°C) (S′/θ′ dissolution)
2618 Al	88.0	238.0	301.0	342.0
2618 + 10	91.0	233.0	287.0	335.0
2618 + 15	91.0	230.0	287.0	327.0

TABLE III Summary of reaction enthalpies associated with each peak in Fig. 2

Material	Reaction enthalpies[a]			
	Peak A (formation) ΔH_{RA} (Jg^{-1})	Peak B (dissolution) ΔH_{RB} (Jg^{-1})	Peak C (formation) ΔH_{RC} (Jg^{-1})	Peak D (dissolution) ΔH_{RD} (Jg^{-1})
2618 Al	7.5	8.2	4.9	7.8
2618 + 10	5.3	10.1	3.5	6.2
2618 + 15	5.3	10.5	3.2	6.0

[a] Based on the average of three integrations.

occurs between 25 and 150 °C for P/M 2124 aluminium and 20 vol% SiC_w/2124 aluminium composite. Peak A is well within these two limits. Hence, this first exothermic peak, A, is attributed to the formation of GPB zones. The curves in Fig. 2 show that the area under the GPB formation peaks (A) for the three materials is different, being smaller for the composites than for the unreinforced matrix. As can be seen, it decreases with alumina particle content. Further, a closer examination shows that the reaction peaks are higher for the composites than for the unreinforced matrix. A summary of all the peak reaction temperatures for the three materials is shown in Table II, for peaks A–D.

An exothermic or endothermic reaction depicts a peak at the temperature at which the reaction is proceeding at its most rapid rate [15, 17, 18] and this temperature is related to the size and stability of the precipitate, and also to the overall reaction kinetics [17, 18]. In particular, the speed with which a precipitation or dissolution reaction takes place is measured by shifts in the temperature peaks. Hence, it is evident that there are two differences between the 2618 control matrix and the matrix of the composites: (i) a decrease of the volume fraction of the GPB zones due to the presence of alumina particles [5], and (ii) a shift in the peak temperatures. This upward shift is interpreted to mean that there are not enough magnesium atoms in the matrix of the composites to enhance precipitation of the GPB zones, although there is a larger density of dislocations in the latter matrix.

The first endothermic reaction, B, based on the above reasoning, is due to the dissolution of GPB zones. The area under the GPB dissolution peak B is larger than the area under the GPB formation peak A for all three materials. This is interpreted to mean that some GPB zones have been precipitated out during quenching from the solution heat-treatment temperature [20]. This, therefore, explains partly why less Mg atoms are available in the composite matrices during the GPB formation reactions.

Further, a visual examination shows that the reaction enthalpy values, ΔH_R, of the GPB dissolution are different for the three materials. A quantitative estimation of this quantity was carried out by means of partial integration of the area under peak B for each material, using the integration software of the thermal analyser. The values are shown in Table III. It is clear that the fraction of GPB dissolved is larger for the composites than for the unreinforced metal matrix. The reaction temperature peaks, T_p, are decreased in the composite materials as compared to that observed in the unreinforced alloy. The results indicate that the GPB dissolution reactions in the composites are expedited by the presence of the alumina particles. Papazian [5] has reported a similar trend for 2124 aluminium reinforced with SiC whiskers but attributed the phenomenon to the powder metallurgy (P/M) route by which the composites were produced.

The heat capacity of alumina is lower than that of aluminium. Therefore, it would take a smaller amount of thermal energy to heat the alumina particles to a temperature sufficiently high to facilitate the dissolution of GPB zones. As such, because the majority of the GPB zones is expected to be situated very close to the alumina–matrix interface, they would tend to heat up and revert faster than those formed in the unreinforced matrix. This phenomenon can produce a shift of the GPB zone dissolution reaction peak to lower temperatures in the composites.

Based on the work of Adler and DeLasi [18], the second exothermic reaction (doublet), labelled C, between 260 and 315 °C is due to the formation of precipitate phases. The first peak is attributed to S′ formation, while the second peak is ascribed to an early formation of the S phase from the S′ precipitates. Another possibility is that the first peak is due to simultaneous formation of S′ and S phases from pre-existing S′, while the second peak is due to the growth of the S phase only [18]. Nevertheless, the existence of the doublet is a strong indication of the formation of two different phases, the confirmation of which can

only be obtained by means of transmission electron microscopy (TEM) or X-ray diffraction (XRD) techniques. Fig. 2 and Table II show that the formation of the S′ phase occurs at lower temperatures in the composites relative to the unreinforced matrix. Thus, the presence of the alumina particles expedited this reaction.

The second endothermic reaction (D) between 315 and 405 °C is attributed to the dissolution of transition (S′) phases. As in the case of the S′ formation reaction, it occurs at lower temperatures in the composite materials than in the unreinforced matrix, indicating that these materials would age faster than their unreinforced counterparts under identical thermal conditions. The third exothermic reaction (E) between 405 and 510 °C is attributed to the formation of the equilibrium S phase, although a separate peak was not observed by Papazian [5] or by Jena *et al.* [20]. The latter investigators have attributed the absence of this peak to the fact that S′ is only a slightly strained version of S which, with increase in temperature, gradually relaxes to become the strain-free S phase. Thompson [16], however, reported the existence of such a peak in Al–4.6% Cu alloy tested under the same as-quenched condition.

3.2.2. Room-temperature ageing

The DSC thermograms of aged samples of the matrix alloy and the composites are shown in Fig. 3. The samples were aged at room temperature for up to 30 days. The peak reaction temperatures, (T_p), for the various phases formed in the three materials are shown in Table IV. The DSC curves indicate that the three materials show the same general reactions. As expected, the volume fraction of the GPB zones formed diminishes with increasing ageing time. After 87 h, the GPB zone formation reactions have

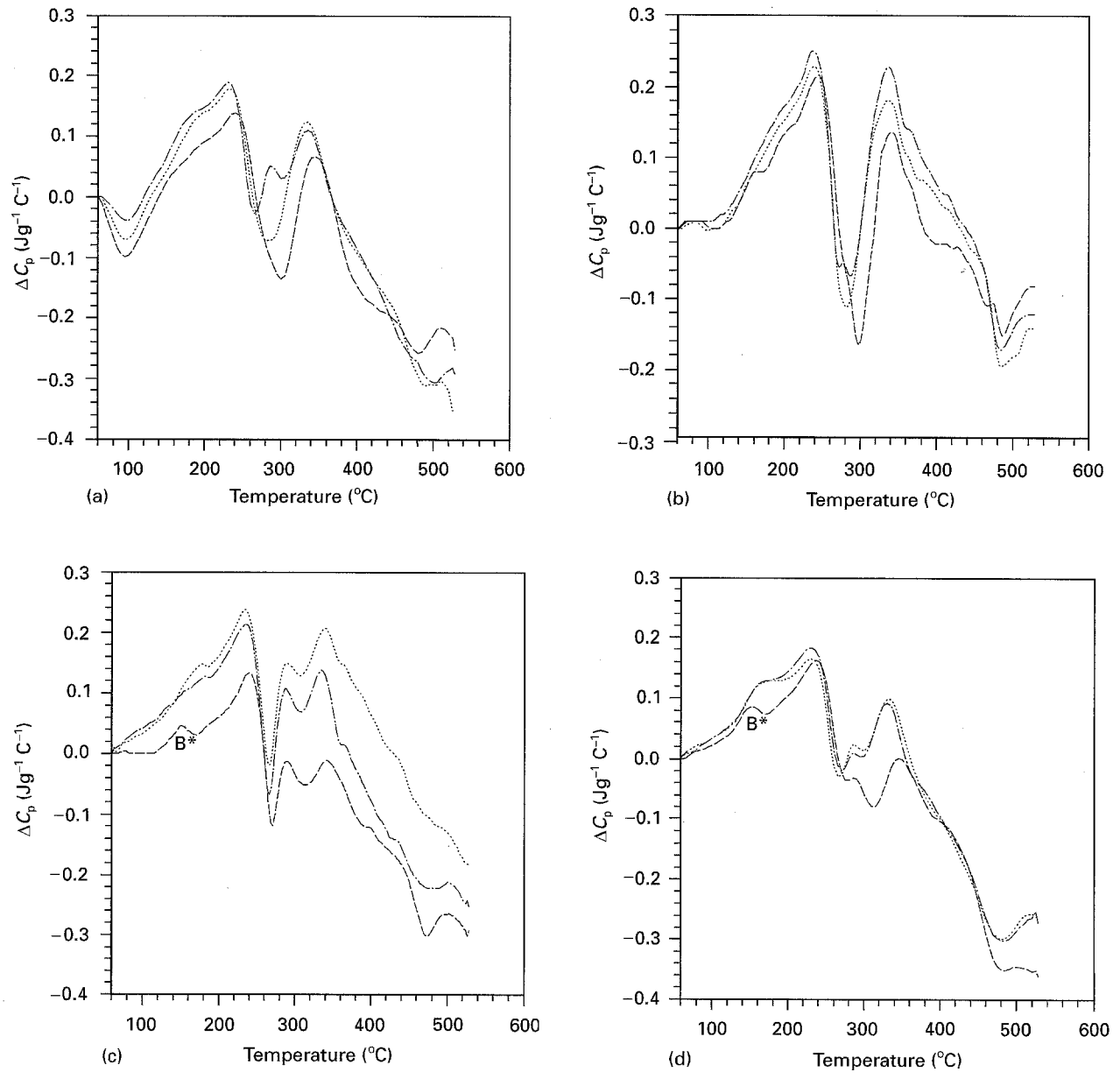

Figure 3 DSC thermograms of the reference alloy and the composites after natural ageing for (a) 18 h; (b) 87 h; (c) 174 h; and (d) 30 d. (– – –) 2618 Al, (-----) 2618 + 10, (– – –) 2618 + 15.

TABLE IV Peak reaction temperatures, T_p, of DSC thermograms for samples aged naturally

Material	Ageing time (h)	Peaks				
		A(°C)	B*(°C)	B(°C)	C(°C)	D(°C)
2618 Al	18	95.0	N/O[a]	240.0	300.0	345.0
2618 + 10	18	95.0	N/O	232.5	282.5	335.0
2618 + 15	18	97.5	N/O	230.0	265.0[c]	335.0
2618 Al	87	–	165.0	245.0	298.0	341
2618 + 10	87	–	N/M[b]	239.0	282.0	337
2618 + 15	87	–	N/M	237.0	272.0[c]	337
2618 Al	174	–	150.0	240.0	270.0	340.0
2618 + 10	174	–	177.0	233.0	266.0	339.0
2618 + 15	174	–	181.0	235.0	266.0	334.0
2618 Al	720	–	152.5	237.0	277.5	345.0
2618 + 10	720	–	172.5	230.0	265.0	332.5
2618 + 15	720	–	172.5	230.0	270.0	330.0

[a] N/O = not observable.
[b] N/M = observed but not measurable.
[c] First peak of the exothermic doublet.

practically ceased in all three materials. However, a new GPB dissolution reaction peak, B*, has become identifiable in the unreinforced alloy, while after 174 h it has become very distinct in the unreinforced alloy and also the composites. The GPB dissolution peak B* was not readily identifiable in the as-quenched condition. Also, it can be observed that peak B* appears at higher temperatures in the composite materials than in the unreinforced matrix for up to the 30 d ageing period. It is believed that some of the GPB zones have stabilized and, therefore, they dissolve at higher temperatures in the temperature range of peak B.

The appearance of peak B* indicates that in 2618 aluminium alloy two types of zones are formed or dissolved after quenching and ageing for a long time at room temperature. This deduction may be rationalized by the fact that the area under the first GPB dissolution peak, B*, is evidently much smaller than that of the GPB zone formation peak, A, at the initial stage of the natural ageing process. Thus, it does not represent the totality of the GPB zone dissolution reactions. The implication is that either all of the GPB zones do not dissolve in the temperature range of B* or another type of zone is formed after a long time of natural ageing. In other words, GPBI zones apparently do not dissolve to form GPBII only because the two-step dissolution peaks are indicative of the presence of another phase. Jena *et al.* [20] have associated the appearance of a peak similar to peak B with the dissolution of GPB zone–dislocation complexes. These complexes were related to the S″ phase which has been reported only by a few investigators [10, 21, 22]. Alekseev *et al.* [10] have recently reported that S″ phases precipitate in the form of thin rods of about 1–2 nm diameter each, uniformly distributed in the matrix alloy, and are accompanied by specific diffraction and thermal effects which distinguish them from other precipitates. If GPBII and S″ phases were distinct phases, the preceding discussion suggests that the decomposition sequence of Al–Cu–Mg alloys would better be described as

$$SSS \rightarrow GPBI \rightarrow GPBII \rightarrow S'' \rightarrow S' \rightarrow S \quad (2)$$

rather than the sequence shown in Equation 1. Otherwise, peak B* is attributed to a different phase, possibly θ'', which is known to occur in Al–Cu alloys or aluminium alloys with low magnesium content. Finally, the reaction temperature peaks, T_p, listed in Table IV show once again that the natural ageing response of the composite materials is enhanced relative to that of the unreinforced alloy.

4. Conclusions

1. The addition of alumina particles does not alter the ageing sequence of 2618 aluminium alloy as demonstrated by the microhardness and DSC results. However, certain aspects of the precipitation reactions are changed due to the presence of the particles.

2. The addition of the alumina particles is found to change the relative quantities of the various phases, in particular, with a decrease in the volume fraction of the GPBI zones.

3. The hardness values of the composite materials are larger than those of the unreinforced alloy during natural ageing, thus suggesting that the strengthening of the composites is influenced by dislocations generated as a result of quenching from the solution heat-treatment temperature.

Acknowledgements

The authors thank Duralcan Aluminium Company, San Diego (USA), for the test materials, and Mr Tom Klimowicz for assistance and technical discussion. Financial assistance from the Natural Sciences and Engineering Research Council of Canada (NSERC) in the form of a research grant to S. Yannacopoulos is acknowledged.

References

1. M. D. SKIBO and S. H. J. LO, in "Proceedings of the International Conference on Composite Materials and Energy (Enercomp 95) ", (Technomic, Lancaster, PA, 1995) p. 563.
2. H. J. RACK, *Adv. Mater. Proc.* **137**(1) (1990) 37.
3. W. C. HARRIGAN, Jr., in "Metal Matrix Composites: Processing and Interfaces", edited by R. K. Everett and R. J. Arsenault (Academic Press, New York, 1991) p. 1.
4. C. ZWEBEN, *J. Metals* **44** (7) (July) (1992) 15.
5. J. M. PAPAZIAN, *Metall. Trans.* **19A** (1988) 2945.
6. S. SURESH, T. CHRISTMAN and Y. SUGIMURA, *Scripta Metall.* **23** (1989) 1599.
7. K. K. CHAWLA and M. METZGER, *J. Mater. Sci.* **7** (1972) 34.
8. R. N. WILSON and P. J. E. FORSYTH, *J. Inst. Metals* **94** (1966) 8.
9. J. M. SILCOCK, *ibid.* **89** (1960–61) 203.
10. A. A. ALEKSEEV, V. N. ANAN'EV, L. B. BER and E. YA KAPUTKIN, *Phys. Metals Metallo.* **75** (1993) 279.
11. A. K. GUPTA, P. GAUNT and M. S. CHATURVEDI, *Philos. Mag.* **55** (1987) 375.
12. K. M. ENTWISTLE, J. H. FELL and K. I. KOO, *J. Inst. Metals* **91** (1962–63) 84.
13. R. N. WILSON and P. G. PARTRIDGE, *Acta Metall.* **13** (1965) 1321.
14. F. P. INCROPERA and D. P. DE WITT, "Fundamentals of Heat Transfer" (Wiley, New York, 1981) p. 763.

15. J. L. PETTY-GALIS and R. D. GOOLSBY, *J. Mater. Sci.* **24** (1989) 1439.
16. D. S. THOMPSON, in "Thermal Analysis", Vol. **2**, edited by R. F. Schwenker Jr. and P. D. Garn (Academic Press, New York, 1969) p. 1147.
17. J. M. PAPAZIAN, *Metall. Trans.* **12A** (1981) 269.
18. P. N. ADLER and R. DELASI, *ibid.* **8A** (1977) 1177.
19. H. K. CHO, *J. Korean Inst. Metals* **10** (1976) 369.
20. A. K. JENA, A. K. GUPTA and M. C. CHATURVEDI, *Acta Metall.* **37** (1989) 885.
21. T. V. SHCHEGOLEVA and N. N. BUINOV, *Fiz. Metall. Metallov.* **23** (1967) 1026.
22. YU. A. BAGARYATSKII, *ibid.* **1** (1955) 316.

Received 8 August
and accepted 21 December 1995